EUROPEAN ORGANIZATION FOR NUCLEAR RESEARCH

CERN-EP/2000-047
March 29, 2000

Search for an invisibly decaying Higgs boson in e^+e^- collisions at $\sqrt{s} = 183 - 189$ GeV

L3 Collaboration

Abstract

A search for a Higgs boson decaying into invisible particles is performed using the data collected at LEP by the L3 experiment at centre-of-mass energies of 183 GeV and 189 GeV. The integrated luminosities are respectively 55.3 pb^{-1} and 176.4 pb^{-1}. The observed candidates are consistent with the expectations from Standard Model processes. In the hypothesis that the production cross section of this Higgs boson equals the Standard Model one and the branching ratio into invisible particles is 100%, a lower mass limit of 89.2 GeV is set at 95% confidence level.

Submitted to *Phys. Lett. B*

1 Introduction

In some extensions of the Standard Model the Higgs boson can decay into stable weakly interacting particles, thus yielding invisible final states [1]. For example the minimal supersymmetric extension of the Standard Model predicts that the Higgs boson can decay into a pair of invisible neutralinos.

A search is performed for a Higgs boson produced through the Higgs-strahlung process, $e^+e^- \to Z^* \to hZ$. The Z boson decays into fermion pairs yielding two different investigated topologies: two acoplanar jets plus missing energy, corresponding to the Z boson hadronic decays, and two acoplanar charged leptons plus missing energy, corresponding to decays of the Z boson into electrons or muons. Data collected by the L3 experiment [2] at LEP centre-of-mass energies of $\sqrt{s} = 183$ GeV and 189 GeV are analysed. The corresponding integrated luminosities are respectively 55.3 pb^{-1} and 176.4 pb^{-1}. Results at lower centre-of-mass energies have been reported by L3 [3] and by the other LEP experiments [4].

2 Event simulation

To determine the signal efficiency, samples of Higgs boson events are generated using the PYTHIA Monte Carlo program [5] for masses between 55 GeV and 100 GeV.

For the background studies the following Monte Carlo programs are used: PYTHIA ($e^+e^- \to q\bar{q}(\gamma)$, $e^+e^- \to Z/\gamma^*Z/\gamma^*$ and $e^+e^- \to Ze^+e^-$), KORALW [6] ($e^+e^- \to W^+W^-$), KORALZ [7] ($e^+e^- \to \mu^+\mu^-(\gamma)$, $e^+e^- \to \tau^+\tau^-(\gamma)$), PHOJET [8] ($e^+e^- \to e^+e^-q\bar{q}$), DIAG36 [9] ($e^+e^- \to e^+e^-\ell^+\ell^-$), BHWIDE [10] ($e^+e^- \to e^+e^-(\gamma)$), and EXCALIBUR [11] for the other four-fermion final states. For each centre-of-mass energy, the number of simulated background events corresponds to at least 50 times the number of expected events except for the two-photon interactions ($e^+e^- \to e^+e^-f\bar{f}$) and Bhabha scattering ($e^+e^- \to e^+e^-$) for which twice and seven times the collected luminosity are simulated, respectively.

The L3 detector response is simulated using the GEANT 3.15 program [12], which takes into account the effects of energy loss, multiple scattering and showering in the detector. The GHEISHA program [13] is used to simulate hadronic interactions in the detector. Small time-dependent inefficiencies of the different subdetectors are taken into account in the simulation procedure.

3 Search in the hadronic channel

A cut-based analysis is used to select events in the hadronic channel. After a common preselection two sequential selections are separately optimised for light (below 80 GeV) and heavy (above 80 GeV) Higgs boson masses. Unless otherwise stated, the events are constrained to have two jets using the DURHAM algorithm [14].

3.1 Preselection

High-multiplicity hadronic events are selected at $\sqrt{s} = 189$ GeV. Events coming from QCD processes and hadronic decays of W and Z boson pairs are rejected by requiring a missing momentum larger than 10 GeV. The absolute values of the cosine of the polar angle of the jets and of the missing momentum vector have to be less than 0.9, to reject events with a

high-energy initial-state radiation photon emitted close to the beam axis. In addition, events with large energy depositions in the forward calorimeters are vetoed to reduce the background contribution from the Ze^+e^- and $q\bar{q}(\gamma)$ processes and from residual two-photon interactions. Coplanar events are rejected to further suppress these last processes.

Events with energetic and isolated charged leptons are removed to decrease the contamination from semi-leptonic decays of W boson pairs. This cut is designed to keep signal events with semi-leptonic decays of b or c hadrons produced in Z decays.

The larger of the jet masses is required to be in the range from 6 GeV up to 50 GeV and the lower one greater than 4 GeV. The upper mass limit further removes some semi-leptonic W boson pair decays and the lower bounds reject two-photon interactions with tau leptons in the final state.

Figure 1 shows the comparison between data and Monte Carlo expectations for the distribution of the visible mass, $M_{\rm vis}$ of the preselected events.

3.2 Heavy Higgs boson selection

In addition to the preselection described above, the correlation between the visible and the missing mass, $M_{\rm mis}$, is used to select heavy Higgs boson candidates in the $\sqrt{s} = 189$ GeV data sample. We define the variable $R = (M_{\rm vis} + M_{\rm mis})/(M_{\rm vis} - M_{\rm mis})$ and we require $R < -3.5$ or $R > 7$, since the signal has a broad R distribution while for the background R is close to zero.

A heavy Higgs boson is characterised by relatively low momentum, hence the missing momentum of the event should not exceed 40 GeV. The background due to the $q\bar{q}(\gamma)$ and two-photon interaction processes is suppressed by rejecting collinear events and by requiring a large value of the event thrust, together with a moderate value of the sum of the inter-jet angles, Θ_{123}, when the events are constrained to have three jets. In order to reject the residual contributions from the W pair and the single W processes, an isolation criterion on the missing momentum vector is applied. In addition, the upper cut on the maximum value of the jet masses is tightened to 30 GeV while the minimum has to be less than 20 GeV.

The recoiling mass, $M_{\rm h}^{rec}$, is calculated by constraining the visible mass to the Z boson mass and imposing energy-momentum conservation [3]; its distribution is plotted in Figure 2(a) for the data and the background. With this kinematical constraint, the recoil mass resolution is 3.5 GeV in the hypothesis of a Higgs boson mass of 90 GeV.

After applying the selection described above the dominant process in the remaining background is the Z boson pair production.

3.3 Light Higgs boson selection

The production of a light invisible Higgs boson at $\sqrt{s} = 189$ GeV is characterised by three main features, exploited by the following selection criteria: mass of the hadronic system close to the Z mass $|M_{\rm vis} - M_{\rm Z}| < 20$ GeV, at least 40% but not more than 60% of the centre-of-mass energy visible in the detector and missing momentum in the window from 30 GeV up to 55 GeV. This last requirement reduces part of the background arising from Z boson pair production and two-photon interactions, the latter being further suppressed by an upper cut on Θ_{123}. Events from $q\bar{q}(\gamma)$ are rejected by requiring a large value of the event thrust and the longitudinal momentum imbalance to be less than 40% of the visible energy. The residual contribution from W pair production is reduced by a cut on the threshold y_{23} at which the DURHAM algorithm resolves the event into three jets from a two-jet topology.

The distribution of $M_{\rm h}^{rec}$ for events selected in the data and the Monte Carlo samples is displayed in Figure 2(b).

The selection of the hadronic channel at $\sqrt{s} = 183$ GeV is similar to this light Higgs boson selection. A cut on the transverse momentum imbalance replaces the cut on the y_{23} parameter and the values of the selection requirements reflect the different centre-of-mass energies. The final $M_{\rm h}^{rec}$ spectrum for data and Monte Carlo is shown in Figure 2(c). Table 1 summarises the yields of all the selections described above.

After applying the two selections described above the dominant process in the remaining background is the $\rm W^+W^-$ production.

	$\sqrt{s} = 189$ GeV			$\sqrt{s} = 183$ GeV
	Preselection	Heavy Higgs boson	Light Higgs boson	Final Selection
Data	304	30	27	8
Background MC	300.3	25.8	23.6	8.5
ϵ (%) ($M_{\rm h} = 65$ GeV)	53.1	3.0	19.2	22.0
ϵ (%) ($M_{\rm h} = 85$ GeV)	54.0	30.2	20.0	28.0
ϵ (%) ($M_{\rm h} = 90$ GeV)	54.1	37.8	7.6	18.5
ϵ (%) ($M_{\rm h} = 95$ GeV)	46.6	32.2	2.1	–

Table 1: Number of events expected from Standard Model processes compared to the number of data events selected by the hadronic selections. The signal efficiencies (ϵ) for several Higgs boson masses $M_{\rm h}$ are also shown.

4 Search in the leptonic channels

The search for an invisibly decaying Higgs boson produced in association with a Z boson decaying into leptons is designed to be almost independent of the Higgs boson mass in the investigated range. Low multiplicity events with a pair of high energy muons or electrons are selected. These are separated from fermion pair production events by requiring large acoplanarity and visible energy between 5% and 70% of the centre-of-mass energy. The lepton energy has to be less than 90% of the beam energy to further reject Bhabha scattering events. Two-photon interactions are suppressed by requiring the lepton pair invariant mass to be larger than 30 GeV and low energy depositions in the forward calorimeters. Events with muons should have at least one scintillator in time with the beam crossing in order to remove cosmic-ray background. The yield of this preselection is presented in Table 2, while Figure 3 displays the spectra of the lepton pair invariant mass, $M_{\ell\ell}$, for data and Standard Model Monte Carlo events.

Residual events due to the radiative return to the Z resonance where the photon remains undetected in the beam pipe are rejected by requiring the missing momentum to point away from the beam axis. Tau pair production can yield acoplanar lepton pairs that satisfy the selection criteria described above. In the hypothesis that the lepton pair originates from a single particle, we require the cosine of the most energetic lepton emission angle θ^* in the Z boson rest frame not to exceed 0.95.

The contribution from two-photon interactions is eliminated by tightening the cut on the lepton invariant masses, 70 GeV $< M_{\ell\ell} <$ 110 GeV; this is also effective against a significant portion of the fully leptonic decays of W bosons. Final states with an electron or muon pair

	Electrons		Muons	
	Preselection	Final selection	Preselection	Final selection
Data	38	2	34	2
Background MC	41.4	2.2	36.5	1.6
ϵ (%) ($M_{\rm h} = 65$ GeV)	52.9	36.5	42.1	19.1
ϵ (%) ($M_{\rm h} = 85$ GeV)	55.4	41.3	42.3	20.9
ϵ (%) ($M_{\rm h} = 90$ GeV)	55.4	39.6	45.8	25.1
ϵ (%) ($M_{\rm h} = 95$ GeV)	55.3	42.1	47.7	30.2

Table 2: Number of events observed and expected from Standard Model processes at $\sqrt{s} = 189$ GeV after the preselections and the final selections. Signal efficiencies (ϵ) for different Higgs mass hypotheses are also shown. The background to the final selected sample is composed of one third Z boson-pair events and two thirds W boson-pair events.

and two neutrinos, produced by Z boson pairs, constitute an irreducible background but their cross section is relatively low.

The visible energy $E_{\rm vis}$, cos θ^*, $M_{\ell\ell}$ and the velocity β of the dilepton system are combined into a single likelihood variable G, defined as:

$$G = \sum_i \log\left(P_S^i(x)\right) - \log\left(P_B^i(x)\right).$$

The index i runs over the four variables and $P_S^i(x)$ and $P_B^i(x)$ are the probability densities for the i-th variable to have a value x in the signal or background hypotheses, respectively. These densities are calculated for each event by interpolating between the two signal Monte Carlo samples whose generated Higgs masses are closer to the event missing mass which is taken as the Higgs boson mass hypothesis. The Z boson pair background is not included in this calculation. Figure 4 shows distributions of G for the data and the expected Monte Carlo background and signal for a Higgs boson mass of 95 GeV.

The number of selected events and the signal efficiency after the optimization [15] of a cut on G are reported in Table 2. The observed resolution on the missing mass is 1.1 GeV in the electron channel, and 5.1 GeV in the muon channel for a Higgs boson mass of 90 GeV.

A cut-based analysis is developed for the $\sqrt{s} = 183$ GeV data sample making use of the following selection criteria: 30 GeV $< E_{\rm vis} <$ 120 GeV, cos $\theta^* < 0.95$, 80 GeV $< M_{\ell\ell} <$ 100 GeV and $0.05 < \beta < 0.55$. In the electron channel, the signal efficiency is 45% and 4 events are observed for 1.4 expected background events. In the muon channel, the signal efficiency is 28% and no events are observed while 1.7 background events are expected. Figure 5 displays the missing mass distributions for the search in the leptonic channel for the combined $\sqrt{s} = 183$ GeV and $\sqrt{s} = 189$ GeV samples.

5 Systematic uncertainties

Two sources of systematic uncertainties, summarised in Table 3, can affect the results. The first is the limited amount of Monte Carlo statistics, which gives the systematic errors on the signal and background efficiencies listed as "MC Stat." in Table 3. The second is the quality of the Monte Carlo description of the background processes. This is studied using data

and Monte Carlo samples containing essentially W^+W^- and ZZ background events. These samples contain about 1100 events for the hadronic channel and 500 for the leptonic ones. The data distributions in these new samples of each selection variable i, except the likelihood G, are compared with those of the Monte Carlo, determining their systematic shifts s_i and the corresponding statistical errors σ_i. All the selection cuts are then shifted by $s_i \pm \sigma_i$, where the sign of σ_i is chosen so as to obtain the lowest efficiency for the single cut on the variable i. The difference between the efficiency of the selection using the shifted cuts and that of the nominal one is taken as the systematic uncertainty. These errors are summarised as "Syst." in Table 3 and are summed in quadrature with the Monte Carlo statistical uncertainties to obtain the total systematic uncertainty, listed as "Total" in Table 3.

	Background			Signal		
	MC Stat.	Syst.	Total	MC Stat.	Syst.	Total
Heavy hadronic	1.0	5.0	5.0	3.0	2.5	4.0
Light hadronic	1.0	5.0	5.0	4.0	5.5	7.0
Electrons	6.0	1.5	6.0	5.0	2.0	5.5
Muons	6.5	5.0	8.0	6.0	3.5	7.0

Table 3: Relative systematic uncertainties in percent on the signal and background efficiencies for each analysis.

6 Results

No indication of the production of a Higgs boson with invisible decays is found. As both the production cross section and the branching ratios are model dependent, it is useful to introduce the ratio $R_{\rm inv} = {\rm BR(h \to \text{invisible particles})} \times \sigma({\rm e^+e^- \to hZ})/\sigma({\rm e^+e^- \to H_{SM}Z})$, where $\rm H_{SM}$ is the Standard Model Higgs boson. A limit on $R_{\rm inv}$ is calculated [16] as a function of the Higgs boson mass making use of the mass distributions presented in Figures 2 and 5. In the determination of the limit the Standard Model Higgs boson cross section as given by the HZHA generator [17] is used and the signal and background efficiencies are lowered by their systematic uncertainties. Results obtained at lower energies [3] are included. Figure 6 shows the 95% confidence level (CL) upper limit on $R_{\rm inv}$ as a function of the Higgs mass $M_{\rm h}$. For the value of $R_{\rm inv} = 1$ the 95% CL lower limit on the Higgs boson mass is:

$$M_{\rm h} > 89.2 \text{ GeV}.$$

The expected lower limit is 92.6 GeV.

Acknowledgements

We wish to express our gratitude to the CERN Accelerator Divisions for the good performance of the LEP machine. We acknowledge the efforts of the engineers and technicians who have participated in the construction and maintenance of this experiment.

Author List

The L3 Collaboration:

M.Acciarri,[26] P.Achard,[19] O.Adriani,[16] M.Aguilar-Benitez,[25] J.Alcaraz,[25] G.Alemanni,[22] J.Allaby,[17] A.Aloisio,[28] M.G.Alviggi,[28] G.Ambrosi,[19] H.Anderhub,[48] V.P.Andreev,[6,36] T.Angelescu,[12] F.Anselmo,[9] A.Arefiev,[27] T.Azemoon,[3] T.Aziz,[10] P.Bagnaia,[35] A.Bajo,[25] L.Baksay,[43] A.Balandras,[4] S.V.Baldew,[2] S.Banerjee,[10] Sw.Banerjee,[10] A.Barczyk,[48,46] R.Barillère,[17] L.Barone,[35] P.Bartalini,[22] M.Basile,[9] R.Battiston,[32] A.Bay,[22] F.Becattini,[16] U.Becker,[14] F.Behner,[48] L.Bellucci,[16] R.Berbeco,[3] J.Berdugo,[25] P.Berges,[14] B.Bertucci,[32] B.L.Betev,[48] S.Bhattacharya,[10] M.Biasini,[32] A.Biland,[48] J.J.Blaising,[4] S.C.Blyth,[33] G.J.Bobbink,[2] A.Böhm,[1] L.Boldizsar,[13] B.Borgia,[35] D.Bourilkov,[48] M.Bourquin,[19] S.Braccini,[19] J.G.Branson,[39] V.Brigljevic,[48] F.Brochu,[4] A.Buffini,[16] A.Buijs,[44] J.D.Burger,[14] W.J.Burger,[32] X.D.Cai,[14] M.Campanelli,[48] M.Capell,[14] G.Cara Romeo,[9] G.Carlino,[28] A.M.Cartacci,[16] J.Casaus,[25] G.Castellini,[16] F.Cavallari,[35] N.Cavallo,[37] C.Cecchi,[32] M.Cerrada,[25] F.Cesaroni,[23] M.Chamizo,[19] Y.H.Chang,[50] U.K.Chaturvedi,[18] M.Chemarin,[24] A.Chen,[50] G.Chen,[7] G.M.Chen,[7] H.F.Chen,[20] H.S.Chen,[7] G.Chiefari,[28] L.Cifarelli,[38] F.Cindolo,[9] C.Civinini,[16] I.Clare,[14] R.Clare,[14] G.Coignet,[4] N.Colino,[25] S.Costantini,[5] F.Cotorobai,[12] B.Cozzoni,[9] B.de la Cruz,[25] A.Csilling,[13] S.Cucciarelli,[32] T.S.Dai,[14] J.A.van Dalen,[30] R.D'Alessandro,[16] R.de Asmundis,[28] P.Déglon,[19] A.Degré,[4] K.Deiters,[46] D.della Volpe,[28] E.Delmeire,[19] P.Denes,[34] F.DeNotaristefani,[35] A.De Salvo,[48] M.Diemoz,[35] M.Dierckxsens,[2] D.van Dierendonck,[2] F.Di Lodovico,[48] C.Dionisi,[35] M.Dittmar,[48] A.Dominguez,[39] A.Doria,[28] M.T.Dova,[18,♯] D.Duchesneau,[4] D.Dufournaud,[4] P.Duinker,[2] I.Duran,[40] H.El Mamouni,[24] A.Engler,[33] F.J.Eppling,[14] F.C.Erné,[2] P.Extermann,[19] M.Fabre,[46] R.Faccini,[35] M.A.Falagan,[25] S.Falciano,[35,17] A.Favara,[17] J.Fay,[24] O.Fedin,[36] M.Felcini,[48] T.Ferguson,[33] F.Ferroni,[35] H.Fesefeldt,[1] E.Fiandrini,[32] J.H.Field,[19] F.Filthaut,[17] P.H.Fisher,[14] I.Fisk,[39] G.Forconi,[14] K.Freudenreich,[48] C.Furetta,[26] Yu.Galaktionov,[27,14] S.N.Ganguli,[10] P.Garcia-Abia,[5] M.Gataullin,[31] S.S.Gau,[11] S.Gentile,[35,17] N.Gheordanescu,[12] S.Giagu,[35] Z.F.Gong,[20] G.Grenier,[24] O.Grimm,[48] M.W.Gruenewald,[8] M.Guida,[38] R.van Gulik,[2] V.K.Gupta,[34] A.Gurtu,[10] L.J.Gutay,[45] D.Haas,[5] A.Hasan,[29] D.Hatzifotiadou,[9] T.Hebbeker,[8] A.Hervé,[17] P.Hidas,[13] J.Hirschfelder,[33] H.Hofer,[48] G. Holzner,[48] H.Hoorani,[33] S.R.Hou,[50] Y.Hu,[30] I.Iashvili,[47] B.N.Jin,[7] L.W.Jones,[3] P.de Jong,[2] I.Josa-Mutuberría,[25] R.A.Khan,[18] M.Kaur,[18,◇] M.N.Kienzle-Focacci,[19] D.Kim,[35] J.K.Kim,[42] J.Kirkby,[17] D.Kiss,[13] W.Kittel,[30] A.Klimentov,[14,27] A.C.König,[30] A.Kopp,[47] V.Koutsenko,[14,27] M.Kräber,[48] R.W.Kraemer,[33] W.Krenz,[1] A.Krüger,[47] A.Kunin,[14,27] P.Ladron de Guevara,[25] I.Laktineh,[24] G.Landi,[16] K.Lassila-Perini,[48] M.Lebeau,[17] A.Lebedev,[14] P.Lebrun,[24] P.Lecomte,[48] P.Lecoq,[17] P.Le Coultre,[48] H.J.Lee,[8] J.M.Le Goff,[17] R.Leiste,[47] E.Leonardi,[35] P.Levtchenko,[36] C.Li,[20] S.Likhoded,[47] C.H.Lin,[50] W.T.Lin,[50] F.L.Linde,[2] L.Lista,[28] Z.A.Liu,[7] W.Lohmann,[47] E.Longo,[35] Y.S.Lu,[7] K.Lübelsmeyer,[1] C.Luci,[17,35] D.Luckey,[14] L.Lugnier,[24] L.Luminari,[35] W.Lustermann,[48] W.G.Ma,[20] M.Maity,[10] L.Malgeri,[17] A.Malinin,[17] C.Maña,[25] D.Mangeol,[30] J.Mans,[34] P.Marchesini,[48] G.Marian,[15] J.P.Martin,[24] F.Marzano,[35] K.Mazumdar,[10] R.R.McNeil,[6] S.Mele,[17] L.Merola,[28] M.Meschini,[16] W.J.Metzger,[30] M.von der Mey,[1] A.Mihul,[12] H.Milcent,[17] G.Mirabelli,[35] J.Mnich,[17] G.B.Mohanty,[10] P.Molnar,[8] B.Monteleoni,[16,†] T.Moulik,[10] G.S.Muanza,[24] A.J.M.Muijs,[2] M.Musy,[35] M.Napolitano,[28] F.Nessi-Tedaldi,[48] H.Newman,[31] T.Niessen,[1] A.Nisati,[35] H.Nowak,[47] G.Organtini,[35] A.Oulianov,[27] C.Palomares,[25] D.Pandoulas,[1] S.Paoletti,[35,17] P.Paolucci,[28] R.Paramatti,[35] H.K.Park,[33] I.H.Park,[42] G.Pascale,[35] G.Passaleva,[17] S.Patricelli,[28] T.Paul,[11] M.Pauluzzi,[32] C.Paus,[17] F.Pauss,[48] M.Pedace,[35] S.Pensotti,[26] D.Perret-Gallix,[4] B.Petersen,[30] D.Piccolo,[28] F.Pierella,[9] M.Pieri,[16] P.A.Piroué,[34] E.Pistolesi,[26] V.Plyaskin,[27] M.Pohl,[19] V.Pojidaev,[27,16] H.Postema,[14] J.Pothier,[17] D.O.Prokofiev,[45] D.Prokofiev,[36] J.Quartieri,[38] G.Rahal-Callot,[48,17] M.A.Rahaman,[10] P.Raics,[15] N.Raja,[10] R.Ramelli,[48] P.G.Rancoita,[26] A.Raspereza,[47] G.Raven,[39] P.Razis,[29] D.Ren,[48] M.Rescigno,[35] S.Reucroft,[11] S.Riemann,[47] K.Riles,[3] A.Robohm,[48] J.Rodin,[43] B.P.Roe,[3] L.Romero,[25] A.Rosca,[8] S.Rosier-Lees,[4] J.A.Rubio,[17] D.Ruschmeier,[8] H.Rykaczewski,[48] S.Saremi,[6] S.Sarkar,[35] J.Salicio,[17] E.Sanchez,[17] M.P.Sanders,[30] M.E.Sarakinos,[21] C.Schäfer,[17] V.Schegelsky,[36] S.Schmidt-Kaerst,[1] D.Schmitz,[1] H.Schopper,[49] D.J.Schotanus,[30] G.Schwering,[1] C.Sciacca,[28] D.Sciarrino,[19] A.Seganti,[9] L.Servoli,[32] S.Shevchenko,[31] N.Shivarov,[41] V.Shoutko,[27] E.Shumilov,[27] A.Shvorob,[31] T.Siedenburg,[1] D.Son,[42] B.Smith,[33] P.Spillantini,[16] M.Steuer,[14] D.P.Stickland,[34] A.Stone,[6] B.Stoyanov,[41] A.Straessner,[1] K.Sudhakar,[10] G.Sultanov,[18] L.Z.Sun,[20] H.Suter,[48] J.D.Swain,[18] Z.Szillasi,[43,¶] T.Sztaricskai,[43,¶] X.W.Tang,[7] L.Tauscher,[5] L.Taylor,[11] B.Tellili,[24] C.Timmermans,[30] Samuel C.C.Ting,[14] S.M.Ting,[14] S.C.Tonwar,[10] J.Tóth,[13] C.Tully,[17] K.L.Tung,[7] Y.Uchida,[14] J.Ulbricht,[48] E.Valente,[35] G.Vesztergombi,[13] I.Vetlitsky,[27] D.Vicinanza,[38] G.Viertel,[48] S.Villa,[11] M.Vivargent,[4] S.Vlachos,[5] I.Vodopianov,[36] H.Vogel,[33] H.Vogt,[47] I.Vorobiev,[27] A.A.Vorobyov,[36] A.Vorvolakos,[29] M.Wadhwa,[5] W.Wallraff,[1] M.Wang,[14] X.L.Wang,[20] Z.M.Wang,[20] A.Weber,[1] M.Weber,[1] P.Wienemann,[1] H.Wilkens,[30] S.X.Wu,[14] S.Wynhoff,[17] L.Xia,[31] Z.Z.Xu,[20] J.Yamamoto,[3] B.Z.Yang,[20] C.G.Yang,[7] H.J.Yang,[7] M.Yang,[7] J.B.Ye,[20] S.C.Yeh,[51] An.Zalite,[36] Yu.Zalite,[36] Z.P.Zhang,[20] G.Y.Zhu,[7] R.Y.Zhu,[31] A.Zichichi,[9,17,18] G.Zilizi,[43,¶] M.Zöller.[1]

1 I. Physikalisches Institut, RWTH, D-52056 Aachen, FRG[§]
III. Physikalisches Institut, RWTH, D-52056 Aachen, FRG[§]
2 National Institute for High Energy Physics, NIKHEF, and University of Amsterdam, NL-1009 DB Amsterdam, The Netherlands
3 University of Michigan, Ann Arbor, MI 48109, USA
4 Laboratoire d'Annecy-le-Vieux de Physique des Particules, LAPP,IN2P3-CNRS, BP 110, F-74941 Annecy-le-Vieux CEDEX, France
5 Institute of Physics, University of Basel, CH-4056 Basel, Switzerland
6 Louisiana State University, Baton Rouge, LA 70803, USA
7 Institute of High Energy Physics, IHEP, 100039 Beijing, China[△]
8 Humboldt University, D-10099 Berlin, FRG[§]
9 University of Bologna and INFN-Sezione di Bologna, I-40126 Bologna, Italy
10 Tata Institute of Fundamental Research, Bombay 400 005, India
11 Northeastern University, Boston, MA 02115, USA
12 Institute of Atomic Physics and University of Bucharest, R-76900 Bucharest, Romania
13 Central Research Institute for Physics of the Hungarian Academy of Sciences, H-1525 Budapest 114, Hungary[‡]
14 Massachusetts Institute of Technology, Cambridge, MA 02139, USA
15 KLTE-ATOMKI, H-4010 Debrecen, Hungary[¶]
16 INFN Sezione di Firenze and University of Florence, I-50125 Florence, Italy
17 European Laboratory for Particle Physics, CERN, CH-1211 Geneva 23, Switzerland
18 World Laboratory, FBLJA Project, CH-1211 Geneva 23, Switzerland
19 University of Geneva, CH-1211 Geneva 4, Switzerland
20 Chinese University of Science and Technology, USTC, Hefei, Anhui 230 029, China[△]
21 SEFT, Research Institute for High Energy Physics, P.O. Box 9, SF-00014 Helsinki, Finland
22 University of Lausanne, CH-1015 Lausanne, Switzerland
23 INFN-Sezione di Lecce and Universitá Degli Studi di Lecce, I-73100 Lecce, Italy
24 Institut de Physique Nucléaire de Lyon, IN2P3-CNRS,Université Claude Bernard, F-69622 Villeurbanne, France
25 Centro de Investigaciones Energéticas, Medioambientales y Tecnologícas, CIEMAT, E-28040 Madrid, Spain[♭]
26 INFN-Sezione di Milano, I-20133 Milan, Italy
27 Institute of Theoretical and Experimental Physics, ITEP, Moscow, Russia
28 INFN-Sezione di Napoli and University of Naples, I-80125 Naples, Italy
29 Department of Natural Sciences, University of Cyprus, Nicosia, Cyprus
30 University of Nijmegen and NIKHEF, NL-6525 ED Nijmegen, The Netherlands
31 California Institute of Technology, Pasadena, CA 91125, USA
32 INFN-Sezione di Perugia and Universitá Degli Studi di Perugia, I-06100 Perugia, Italy
33 Carnegie Mellon University, Pittsburgh, PA 15213, USA
34 Princeton University, Princeton, NJ 08544, USA
35 INFN-Sezione di Roma and University of Rome, "La Sapienza", I-00185 Rome, Italy
36 Nuclear Physics Institute, St. Petersburg, Russia
37 INFN-Sezione di Napoli and University of Potenza, I-85100 Potenza, Italy
38 University and INFN, Salerno, I-84100 Salerno, Italy
39 University of California, San Diego, CA 92093, USA
40 Dept. de Fisica de Particulas Elementales, Univ. de Santiago, E-15706 Santiago de Compostela, Spain
41 Bulgarian Academy of Sciences, Central Lab. of Mechatronics and Instrumentation, BU-1113 Sofia, Bulgaria
42 Laboratory of High Energy Physics, Kyungpook National University, 702-701 Taegu, Republic of Korea
43 University of Alabama, Tuscaloosa, AL 35486, USA
44 Utrecht University and NIKHEF, NL-3584 CB Utrecht, The Netherlands
45 Purdue University, West Lafayette, IN 47907, USA
46 Paul Scherrer Institut, PSI, CH-5232 Villigen, Switzerland
47 DESY, D-15738 Zeuthen, FRG
48 Eidgenössische Technische Hochschule, ETH Zürich, CH-8093 Zürich, Switzerland
49 University of Hamburg, D-22761 Hamburg, FRG
50 National Central University, Chung-Li, Taiwan, China
51 Department of Physics, National Tsing Hua University, Taiwan, China

§ Supported by the German Bundesministerium für Bildung, Wissenschaft, Forschung und Technologie
‡ Supported by the Hungarian OTKA fund under contract numbers T019181, F023259 and T024011.
¶ Also supported by the Hungarian OTKA fund under contract numbers T22238 and T026178.
♭ Supported also by the Comisión Interministerial de Ciencia y Tecnología.
♯ Also supported by CONICET and Universidad Nacional de La Plata, CC 67, 1900 La Plata, Argentina.
♢ Also supported by Panjab University, Chandigarh-160014, India.
△ Supported by the National Natural Science Foundation of China.
† Deceased.

References

[1] K. Griest and H.E. Haber, Phys. Rev. **D 37** (1998) 719; A. Djouadi *et al.* Phys. Lett. **B 376** (1996) 220.

[2] L3 Collab., B. Adeva *et al.*, Nucl. Instr. Meth. **A 289** (1990) 35; J.A. Bakken *et al.*, Nucl. Instr. Meth. **A 275** (1989) 81; O. Adriani *et al.*, Nucl. Instr. Meth. **A 302** (1991) 53; B. Adeva et al., Nucl. Instr. Meth. **A 323** (1992) 109; K. Deiters *et al.*, Nucl. Instr. Meth. **A 323** (1992) 162; M. Chemarin *et al.*, Nucl. Instr. Meth. **A 349** (1994) 345; M. Acciarri *et al.*, Nucl. Instr. Meth. **A 351** (1994) 300; G. Basti *et al.*, Nucl. Instr. Meth. **A 374** (1996) 293; A. Adam *et al.*, Nucl. Instr. Meth. **A 383** (1996) 342.

[3] L3 Collab., M. Acciarri et al., Phys. Lett. **B 418** (1997) 389.

[4] ALEPH Coll., R. Barate *et al.*, Phys. Lett. **B 450** (1999) 301; DELPHI Collab., P. Abreu *et al.*, Phys. Lett. **B 459** (1999) 367; OPAL Collab., G. Abbiendi *et al.*, Eur. Phys. J. **C 7** (1999) 407.

[5] T. Sjöstrand, preprint CERN-TH/7112/93 (1993), revised August 1995; T. Sjöstrand, Comp. Phys. Comm. **82** (1994) 74.

[6] M. Skrzypek *et al.*, Comp. Phys. Comm. **94** (1996) 216; M. Skrzypek *et al.*, Phys. Lett. **B 372** (1996) 289.

[7] S. Jadach, B.F.L. Ward, Z. Wąs, Comp. Phys. Comm. **79** (1994) 503.

[8] R. Engel, Z. Phys. **C 66** (1995) 203; R. Engel, J. Ranft and S. Roesler, Phys. Rev. **D 52** (1995) 1459.

[9] F.A. Berends, P.H. Daverfeldt, R. Kleiss, Nucl. Phys. **B 253** (1985) 441.

[10] S. Jadach, W. Placzeck, B.F.L. Ward, Phys. Rev. **D 40** (1989) 3582; Comp. Phys. Comm. **70** (1992) 305; Phys. Lett. **B 390** (1997) 298.

[11] F.A. Berends, R. Kleiss and R. Pittau, Comp. Phys. Comm. **85** (1995) 447.

[12] R. Brun *et al.*, preprint CERN DD/EE/84-1 (Revised 1987).

[13] H. Fesefeldt, RWTH Aachen Report PITHA 85/02 (1985).

[14] S. Catani *et al.*, Phys. Lett. **B 269** (1991) 432; S. Bethke *et al.*, Nucl. Phys. **B 370** (1992) 310.

[15] J.F. Grivaz and F. Le Diberder, preprint LAL-92-37 (1992).

[16] A. Favara and M. Pieri, preprint hep-ex/9706016 (1997).

[17] P. Janot, "The HZHA generator", in "Physics at LEP2", Eds. G. Altarelli, T. Sjöstrand and F. Zwirner, CERN 96-01 (1996) Vol.2, 309.

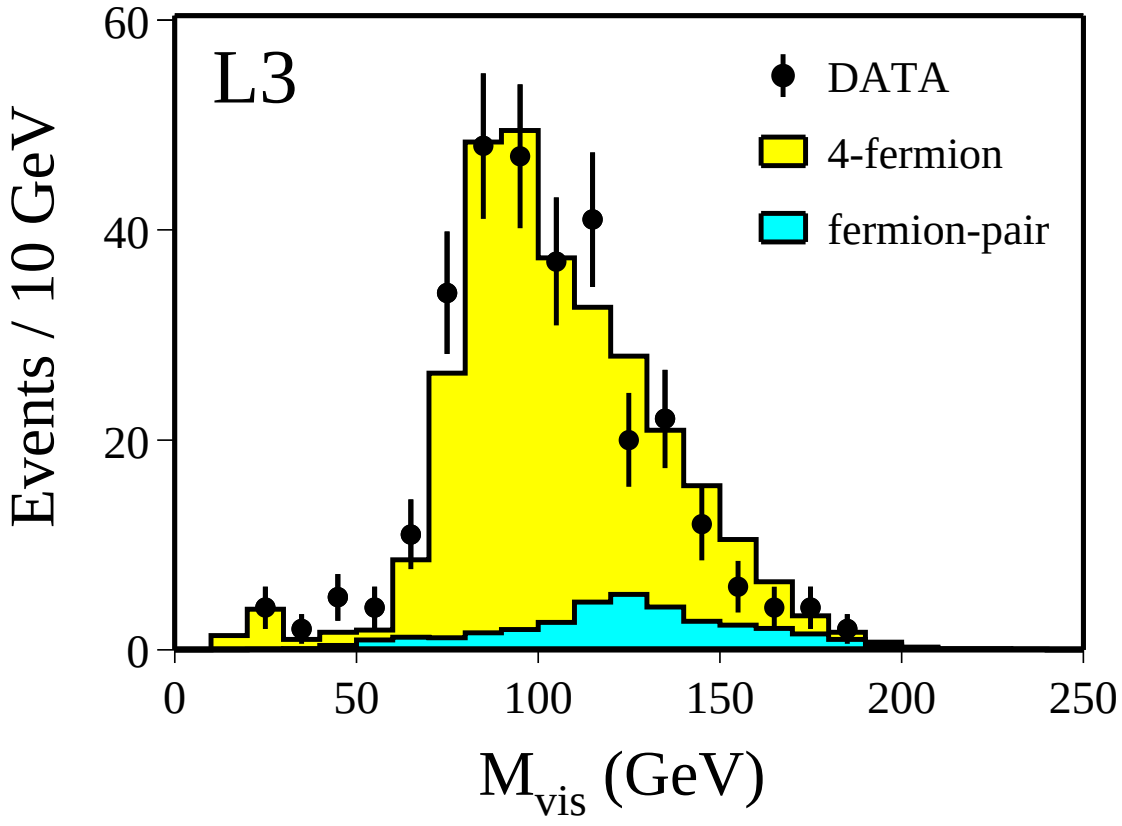

Figure 1: The distribution of the visible mass after the hadronic preselection at $\sqrt{s} = 189$ GeV.

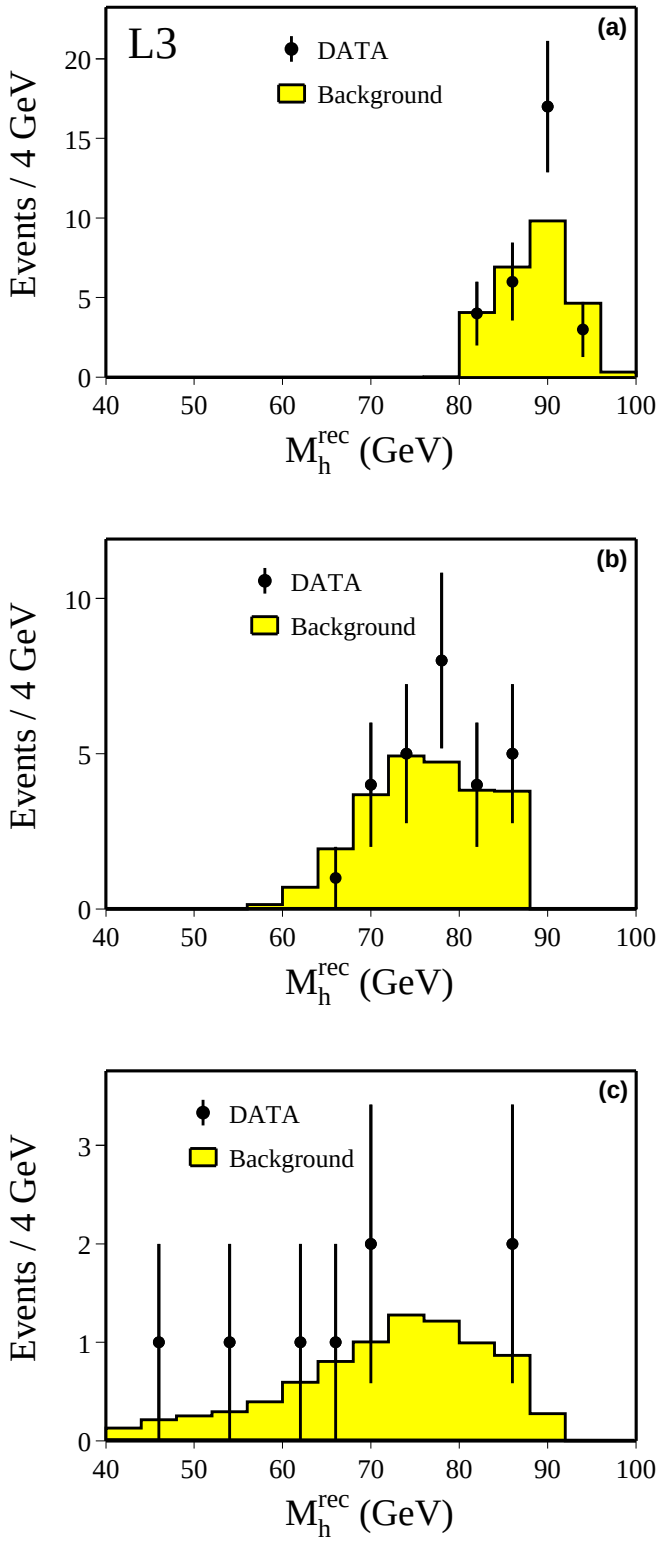

Figure 2: The distribution of the recoil mass (a) after the heavy Higgs boson selection at $\sqrt{s} = 189$ GeV, (b) after the light Higgs boson selection at $\sqrt{s} = 189$ GeV and (c) after the final selection at $\sqrt{s} = 183$ GeV.

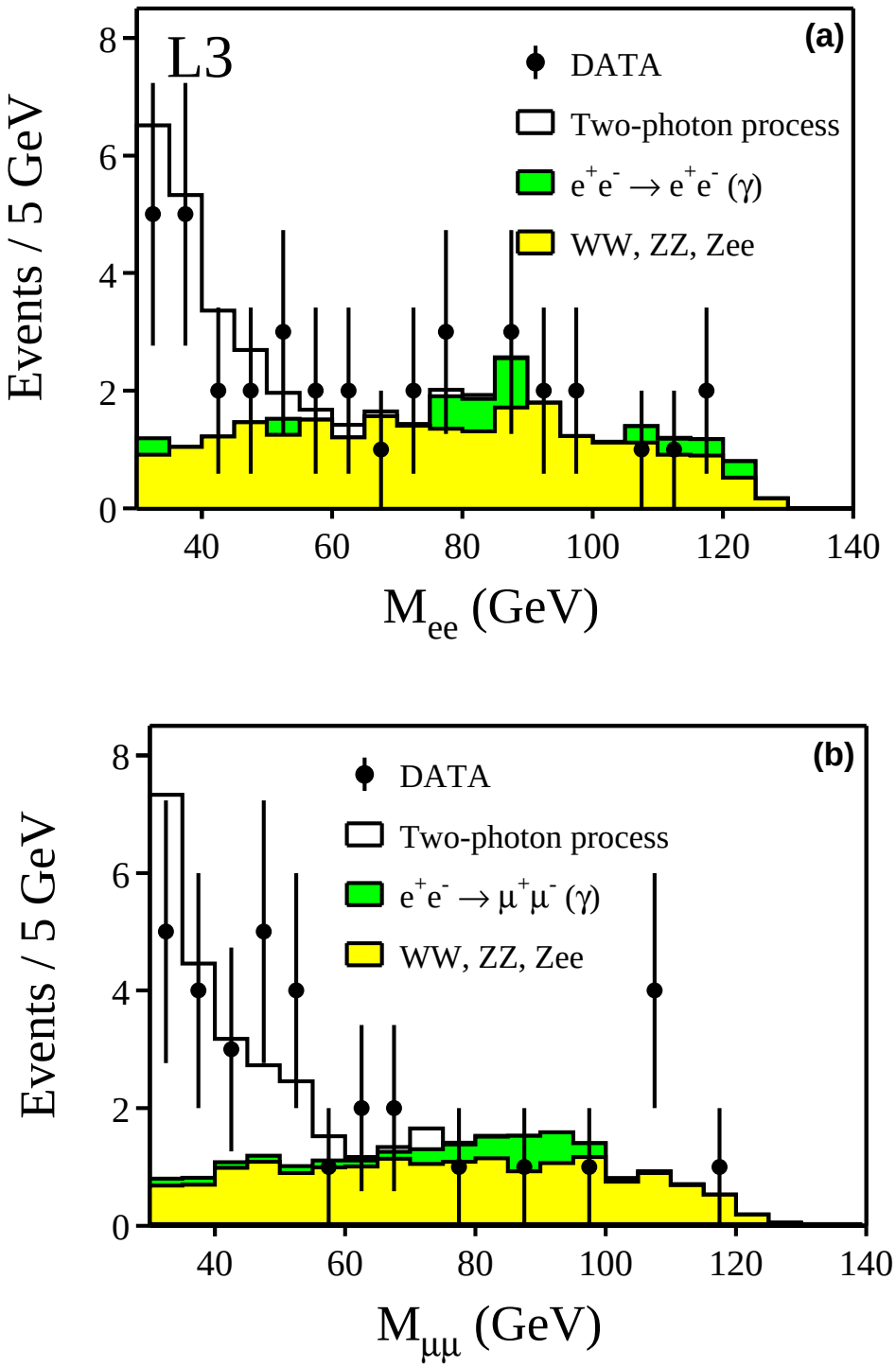

Figure 3: Distribution of (a) the dielectron and (b) the dimuon invariant mass at $\sqrt{s} = 189$ GeV after the preselection is applied.

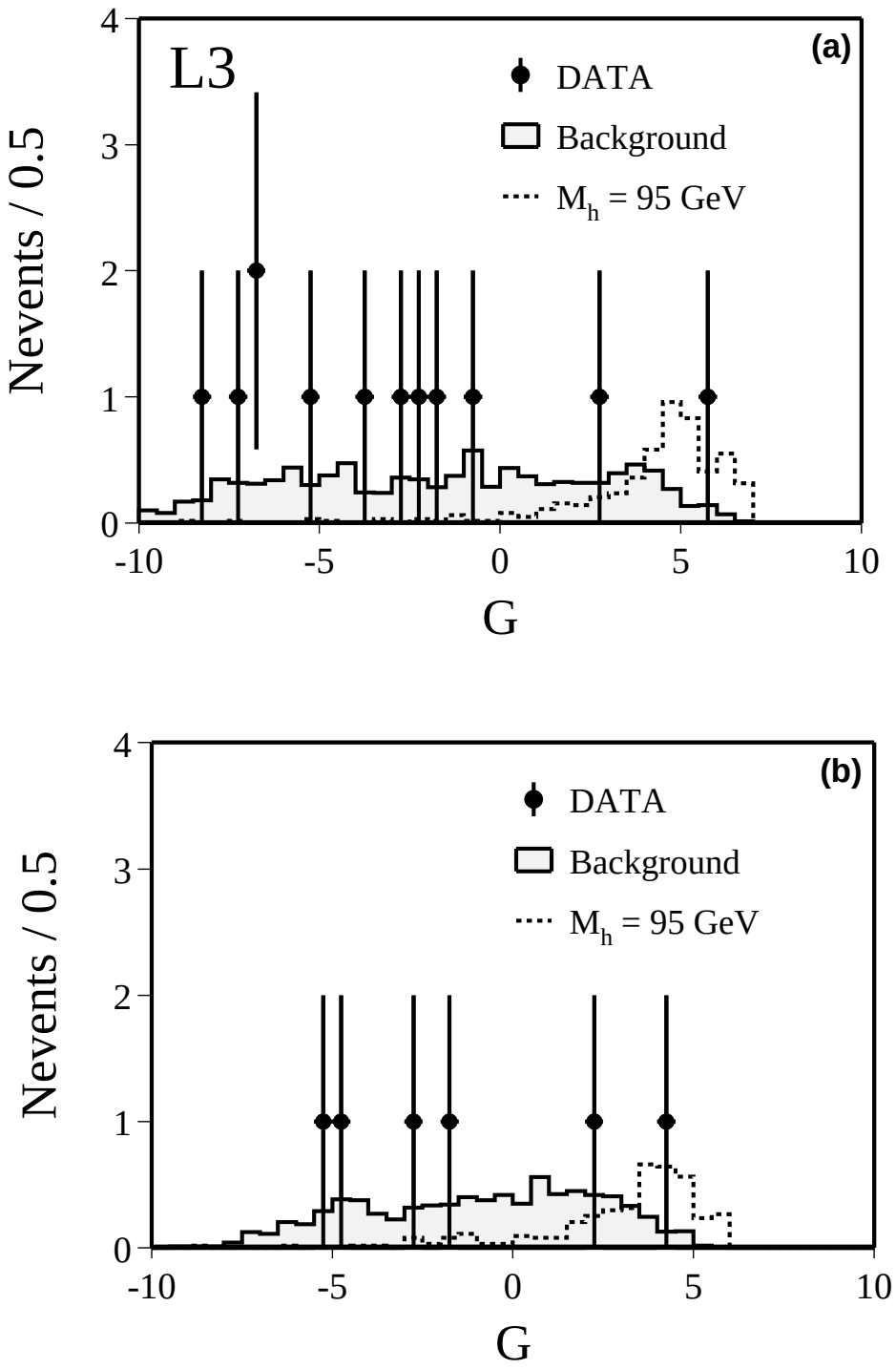

Figure 4: Distributions of the final likelihood variable, G, (a) for the electron and (b) for the muon selections at $\sqrt{s} = 189$ GeV, for data and the expected background. A possible Higgs signal ($M_{\rm h} = 95$ GeV) with an arbitrary cross section is also shown.

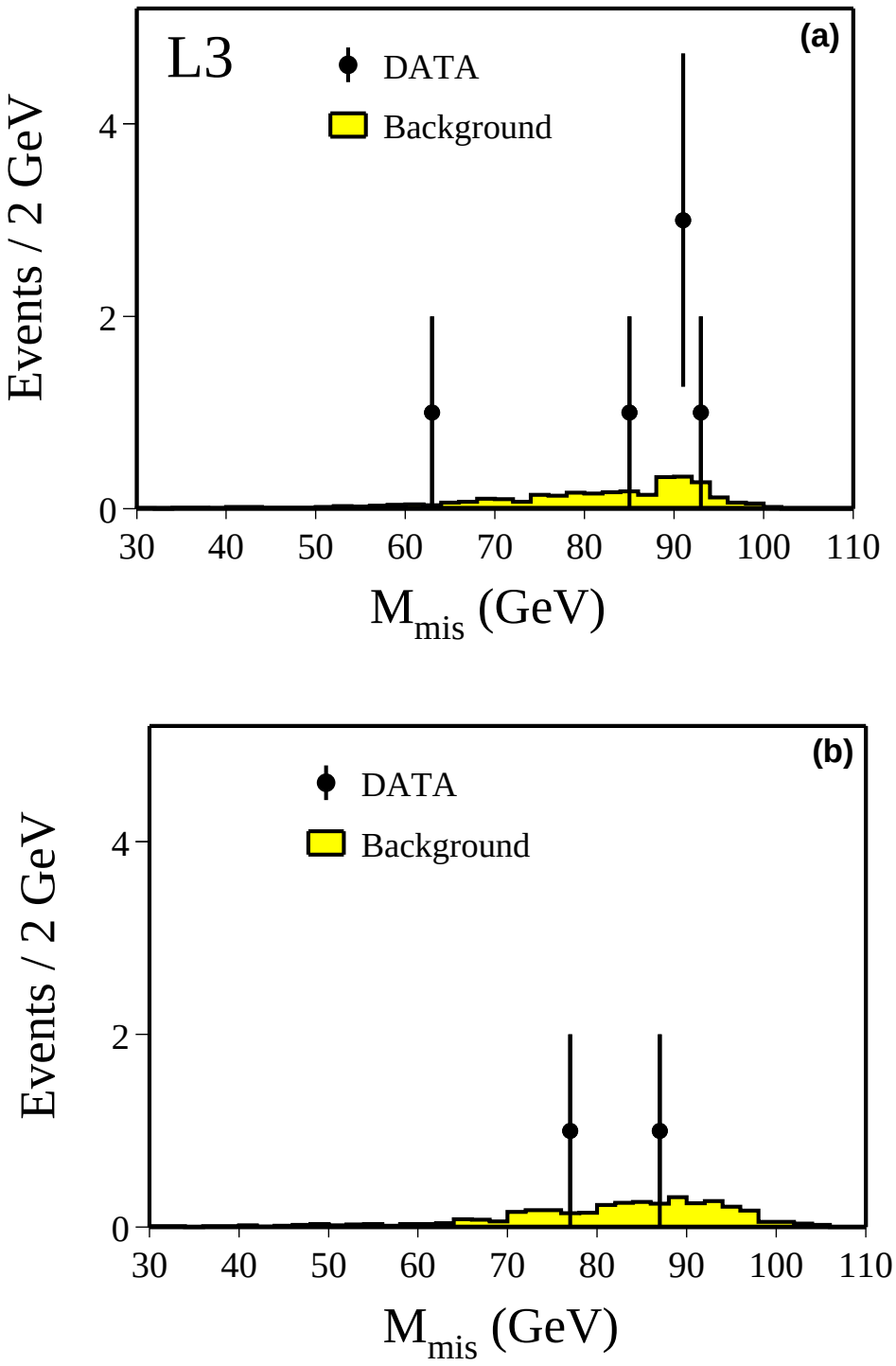

Figure 5: The missing mass distributions (a) in the electron channel and (b) in the muon channel for the combined $\sqrt{s} = 183$ GeV and 189 GeV data samples.

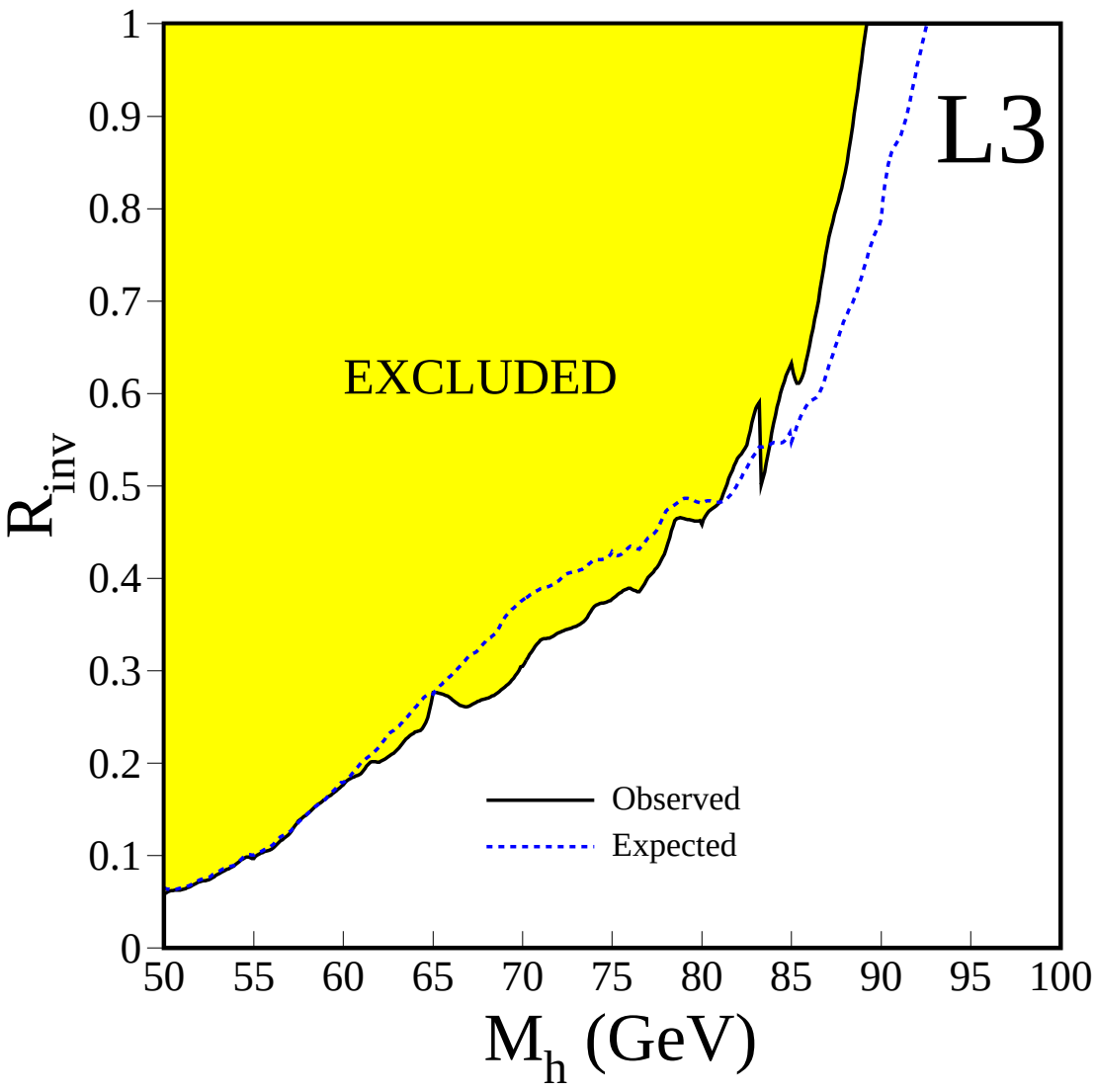

Figure 6: Observed and expected upper limits on the ratio of the invisibly-decaying Higgs boson cross section to that of the Standard Model Higgs boson, as function of the Higgs boson mass. The shaded area is excluded at least at 95% confidence level.